A&A 485, 865–869 (2008)
DOI: 10.1051/0004-6361:200809704

Astronomy & Astrophysics

Rayleigh scattering by H_2 in the extrasolar planet HD 209458b

A. Lecavelier des Etangs[1,2], A. Vidal-Madjar[1,2], J.-M. Désert[1,2], and D. Sing[1,2]

[1] CNRS, UMR 7095, Institut d'Astrophysique de Paris, 98bis boulevard Arago, 75014 Paris, France
e-mail: lecaveli@iap.fr
[2] UPMC Univ. Paris 6, UMR 7095, Institut d'Astrophysique de Paris, 98bis boulevard Arago, 75014 Paris, France

Received 3 March 2008/ Accepted 8 April 2008

ABSTRACT

Transiting planets, such as HD 209458b, offer a unique opportunity to scrutinize the planetary atmospheric content. Although molecular hydrogen is expected to be the main atmospheric constituent, H_2 remains uncovered because of the lack of strong transition from near-ultraviolet to near-infrared. Here we analyse the absorption spectrum of HD 209458b obtained by Sing et al. (2008a, ApJ, submitted) which provides a measurement of the absorption depth in the 3000−6200 Å wavelength range. We show that the rise in absorption depth at short wavelengths can be interpreted as Rayleigh scattering within the atmosphere of HD 209458b. Since Rayleigh scattering traces the entire atmosphere, this detection enables a direct determination of the pressure-altitude relationship, which is required to determine the absolute fraction of other elements such as sodium. At the zero altitude defined by the absorption depth of 1.453%, which corresponds to a planetary radius of 0.1205 times the stellar radius, we find a pressure of 33 ± 5 mbar. Using the variation of the Rayleigh scattering cross-section as a function of wavelength, we determine the temperature to be 2200 ± 260 K at 33 mbar pressure.

Key words. stars: planetary systems

1. Introduction

Transiting planets such as HD 209458b provide a unique opportunity to scrutinize their atmospheric content (e.g., Charbonneau et al. 2002; Vidal-Madjar et al. 2003, 2004, 2008; Ballester et al. 2007; Barman 2007; Lecavelier des Etangs 2007; Ehrenreich et al. 2008). The theory of transmission spectroscopy was developed in detail by the pioneering works of Saeger & Sasselov (2000), Brown (2001), and Hubbard et al. (2001). Primary transits can reveal minute quantities of gas through spectral absorption leading to larger apparent planet size, or larger absorption depth in the transit light curve, at wavelengths characteristic of the absorber. Due to Rayleigh scattering, the main atmospheric constituent, H_2, is seen by means of the ramp-up of apparent planetary radius from 500 to 300 nm (Hubbard et al. 2001). Using transmission spectroscopy, several minor constituents of the atmosphere of HD 209458b have already been uncovered, including sodium, atomic hydrogen, carbon and oxygen.

The extrasolar planet HD 209458b was observed during primary transit using the *Hubble Space Telescope* STIS instrument, at low resolving power using the G430L and G750L spectrograph, and at medium resolution using the G750M spectrograph. The data was analyzed as described in Balleter et al. (2006) and Sing et al. (2008a); special care was taken to correct for the limb-darkening effect. In this article, we use the absorption depth (AD) of the planet, which was measured as a function of wavelength from 3000 Å to ~6200 Å.

In the whole paper, the zero altitude in the planet atmosphere is defined to be the mean absorption depth of 1.453%, measured by Knutson et al. (2007). This corresponds to a planetary radius of 0.1205 times the stellar radius.

In Sect. 2, we present first estimates of temperature and pressure that can be obtained assuming that the Rayleigh scattering by molecular hydrogen is responsible for the observed increase in absorption depth at short wavelengths. In Sect. 3, we present a fit to the data including Na I absorption lines. Discussion and conclusion can be found in Sects. 4 and 5.

2. First estimates

2.1. The HD 209458b transit spectrum from 3000 to 6200 Å

In a plot of the absorption depth as a function of wavelength, an increase in absorption depth is observed toward shortest wavelengths below ~5000 Å (Fig. 1). Above 5000 Å, the absorption depth remains roughly constant up to 5500 Å, before rising again from 5500 to 6000 Å. This last increase in absorption depth, which has a maximum at about 5900 Å is interpreted to be due to a high abundance of sodium in the bottom atmosphere, below the Na_2S cloud level (Sing et al. 2008b).

In the short wavelength side, the mean absorption depth is measured to be 1.444%+/−0.002% between 4500 and 5500 Å, while it is 1.475% ± 0.005% between 3000 and 3900 Å. This significant variation of 0.030% in absorption depth was already identified in the same dataset (Ballester et al. 2007). Ballester et al. (2007) proposed that the increase in absorption depth *below 4000 Å* could be due to absorption in the Balmer series by an optically thin layer of excited hydrogen atoms at high altitude in the planetary atmosphere. Here we propose another explanation: Rayleigh scattering.

2.2. Rayleigh scattering

Following the derivation of Lecavelier des Etangs et al. (2008), we define $\tau_{\rm eq}$ as the optical depth at the altitude $z_{\rm eq}$, such that a sharp occulting disk of radius $R_{\rm p}+z_{\rm eq}$ produces the same absorption depth (AD) as the planet with a translucent atmosphere. In

other words, τ_{eq} is defined to be $AD = (R_p + z(\tau = \tau_{eq}))^2/R_{star}^2$, where R_p and R_{star} are the planet and star radii, respectively. Numerical integration of absorption depth from model atmospheres shows that τ_{eq} is quasi-constant; its value is ∼0.56 for a wide range of atmospheric scale height, H, provided R_p/H is between ∼30 and ∼3000 (Lecavelier des Etangs et al. 2008). For a temperature T, the atmosphere scale height is given by $H = kT/\mu g$, where g is the gravity and μ is the mean molecular mass. In the case of HD 209458b, R_p/H varies between 100 and 1000, when the temperature varies from 300 to 3000 K. For a given atmospheric structure and composition, the theoretical absorption depth at a wavelength λ can be therefore calculated by finding $z(\tau = \tau_{eq}, \lambda)$, which solves the equation $\tau(z, \lambda) = \tau_{eq} = 0.56$ (for details, see Lecavelier et al. 2008).

The Rayleigh scattering cross-section follows a power-law function of wavelength to the power of four, of the form: $\sigma(\lambda) = \sigma_0(\lambda/\lambda_0)^{-4}$, where σ_0 is the Rayleigh scattering cross-section at a reference wavelength λ_0. The high value of exponent in the power law is the reason behind the Earth's blue sky. In this case, equations from Lecavelier des Etangs et al. (2008) that give the planet radius as a function of the wavelength can be solved analytically. For the absorption depth of Rayleigh scattering, this leads to the simple equation

$$AD = AD_0 \left(1 - \frac{8H}{R_p} \ln \frac{\lambda}{\lambda_0}\right), \quad (1)$$

where AD_0 is the absorption depth at a reference wavelength λ_0.

Two important quantities appear in this equation. First, the absorption depth follows a linear relation as a function of the logarithm of wavelength; the slope is characteristic of the scale height H, which is directly proportional to the temperature. Second, the total density and therefore the pressure at the altitude defined by AD_0 corresponds to density and pressure at which Rayleigh scattering is opaque at wavelength λ_0. Thus, the determination of the couple (AD_0, λ_0) provides an absolute reference for the altitude-pressure relationship. This absolute reference is required to interpret measurements of relative absorption depth by minor species such as sodium, and to determine their abundances (Sing et al. 2008b).

The temperature is directly related to the observed variation in absorption depth as a function of wavelength. For HD 209458b, assuming a temperature of 1500 K that provides a typical scale height of 550 km with the planetary parameters of Knutson et al. (2007), and using a mean molecular mass of $\mu = 2.3\ m_p$, where m_p is the mass of the proton, the variation in absorption depth is expected to be to be −0.034% from 3000 Å to 5000 Å; this is similar to what is observed in the G430L data. In the other way, if interpreted in term of Rayleigh scattering, the observed increase in absorption depth at short wavelengths of 0.031% between 3500 and 5000 Å (Sect. 1) implies a temperature of about 2000 K.

Concerning the pressure, the fit of the measured absorption depth from 3200 to 5000 Å by the law given in Eq. (1) provides $AD_0 = 1.453\%$ at $\lambda_0 = 4300$ Å, where 1.453% corresponds to the mean planet radius measured by Knutson et al. (2007). This allows the derivation of the pressure at the planet radius (zero altitude) to be $P_0 = \tau_{eq}/\sigma_0 \times \sqrt{kT\mu g/2\pi R_p}$, where σ_0 is the Rayleigh scattering cross-section at 4300 Å (Lecavelier des Etangs et al. 2008). Using the refractive index of molecular hydrogen $(r - 1) = 1.32 \times 10^{-4}$, one derives $\sigma_0 = 2.3 \times 10^{-27}$ cm^2 at $\lambda_0 = 4300$ Å, and $P_0 \sim 30$ mbar.

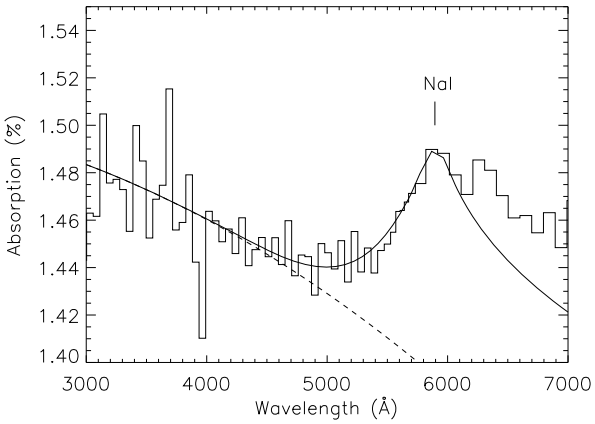

Fig. 1. Plot of absorption depth as a function of wavelength (histogram). The data were rebinned by 20 pixels corresponding to 55 Å per bin at wavelengths below 5500 Å. The measured absorption depths have typical 1-σ error bars of 0.015% to 0.020% per bin below 4000 Å, and about 0.010% above 4500 Å. The thick line shows the best fit to the data using the temperature-pressure-altitude profile given in Sing et al. (2008b). The dashed line shows the absorption with Rayleigh scattering only.

3. Fit of the spectrum

3.1. Fit with Rayleigh scattering and sodium line

Beyond simple estimates using a model that includes only Rayleigh scattering, we can measure the atmospheric structure of HD 209458b more accurately using a global fit to the data which introduces other absorbents, and includes medium-resolution data which further constrains the characteristics of sodium in the high atmosphere (Sing et al. 2008b). With other absorbents, the absorption depth cannot be calculated analytically and a numerical fit to the data is required.

We fit the whole set of data, including data acquired using the medium resolution G750M spectrograph (Sing et al. 2008a,b). In the fit, the pressure and temperature profile as a function of altitude, as well as the sodium abundance, are free parameters. There is a total of 7 free parameters that are described in Sing et al. (2008b): five parameters describe the $T - P$ profile and two parameters, the sodium abundance below and above the sodium condensation temperature. The sodium absorption line profile is calculated using collisional broadening (Iro et al. 2005). We obtain a satisfactory fit, which has a χ^2 of 40 for 52 degrees of freedom in the low-resolution data set (Fig. 1). The results for sodium clouds and the corresponding temperature-pressure diagram are given and discussed in Sing et al. (2008b).

Defining zero altitude to be an absorption depth of 1.453%, we find that the temperature and pressure at this altitude are constrained mainly by Rayleigh scattering below 5000 Å. We find $P_0 = 33 \pm 5$ mbar and $T_0 = 2200 \pm 260$ K (1-σ). At this pressure and temperature, the Rayleigh scattering makes the atmosphere optically thick at wavelength shorter than ∼5000 Å, and causes a significant increase in the absorption depth of ∼0.03% from 5000 Å to 3000 Å (Fig. 1). The blue wing of the sodium line overcomes the absorption due to Rayleigh scattering at wavelengths longer than ∼5000 Å. An additional absorption in the red wing of the sodium line, beyond 6200 Å, could be explained by TiO and VO molecules (Désert et al., in preparation). The sodium abundance required to fit the blue tail of the line profile is found to be $X(\mathrm{NaI}) = 4.3^{+2.1}_{-1.3} \times 10^{-6}$, which is two to four times the solar abundance (Asplund el al. 2005).

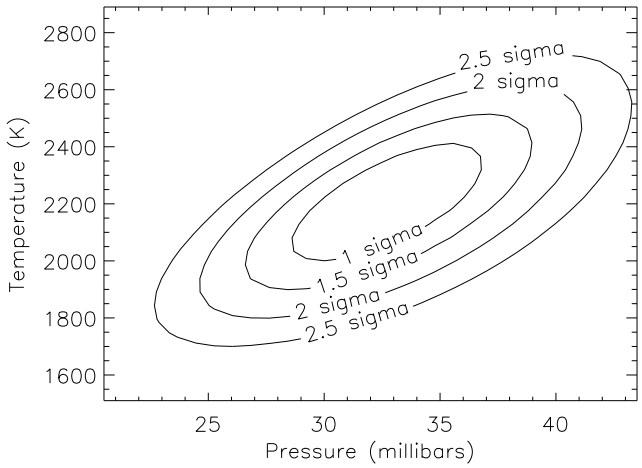

Fig. 2. Plot of error bars for the temperature and the pressure at the zero altitude level corresponding to the altitude at which the absorption depth is 1.453%.

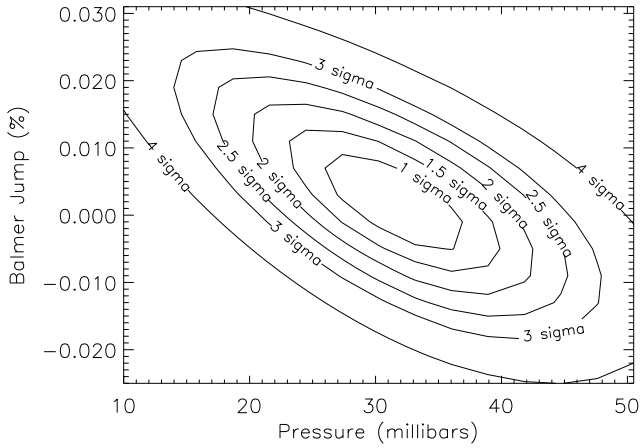

Fig. 3. Plot of error bars for the pressure and the Balmer increment ($\Delta AD_{\rm Balmer}$). This shows that a sharp increase in absorption depths at the limit of the Balmer series is not significantly detected. The increase in absorption depth of ~0.030% is more likely to be due to Rayleigh scattering by gas at ~33 mbar pressure than by a Balmer jump of ~0.030%.

Error bars for temperature and pressure at the zero altitude level, are plotted in Fig. 2. These error bars are calculated using the χ^2 difference between the data and a fit to the absorption depth measurements from 3200 to 6200 Å. For a given temperature and pressure at zero altitude, the other parameters of the fit are free to vary. Therefore, the resulting error bars include the uncertainties in the sodium abundance and other parameters of the $T - P$ profile.

This fit to the data does not assume an isothermal temperature profile as function of altitude in the atmosphere. Even more, the temperature gradient is found to be large and close to the limit allowed by the adiabatic gradient (Sing et al. 2008b). An isothermal assumption is used only to calculate the column density in the limb grazing line of sight. Following Fortney (2005), we used an isothermal decrease of density with altitude to derive an approximation of the column density, $N_{\rm iso} = n\sqrt{2\pi HR_{\rm p}}$, where n is the volume density at lowest altitude in the line of sight (see also Lecavelier des Etangs et al. 2008). With a temperature gradient $\mathrm{d}T/\mathrm{d}z$, a better approximation of the column density is given by $N \approx N_{\rm iso}\sqrt{T\mathrm{d}z/H\mathrm{d}T}\,\Gamma(1/2 + T\mathrm{d}z/H\mathrm{d}T)/\Gamma(1 + T\mathrm{d}z/H\mathrm{d}T)$, that is $N \approx N_{\rm iso}(1-0.125H\mathrm{d}T/T\mathrm{d}z)$. For the maximum temperature gradient that corresponds to the onset of convection (adiabatic $T-P$ profile) and is given by $H\mathrm{d}T/T\mathrm{d}z = 2/7$, the difference between $N_{\rm iso}$ and the actual column density is less than 4%. The results provided here are thus unaffected by the actual shape of the temperature profile.

3.2. Alternative scenario

3.2.1. Balmer jump

The rise of absorption depth at short wavelengths has already been interpreted in terms of an extended cloud of excited hydrogen that is optically thin at wavelengths shorter than the Balmer limit (Ballester et al. 2007). To analyze this possibility, we add one free parameter to the model with a jump in absorption depth between 3600 and 3900 Å, $\Delta AD_{\rm Balmer}$. The additional absorption is taken to be zero above 3900 Å and linearly increases to reach $\Delta AD_{\rm Balmer}$ at 3600 Å and below. A fit to the data using this additional free parameter provides $\Delta AD_{\rm Balmer} = 0.002\% \pm 0.007\%$. The best fit corresponds to a χ^2 of 40, while a Balmer increment of ~0.030% as claimed by Ballester et al. (2007) increases the χ^2 to ≳50 and decreases the pressure at zero altitude to ~15 mbar to avoid absorption by Rayleigh scattering (Fig. 3). We therefore conclude that Rayleigh scattering with a smooth increase in absorption depth at short wavelengths better fit the observational data than the "Balmer jump" with its sharp increase in absorption depth below ~4000 Å.

Alternatively, the "Balmer jump" in absorption due to a cloud of excited hydrogen could also be consistent with the measurements, if we consider an additional absorber to explain the low variation in absorption depth between 4000 and 5000 Å. Therefore, we add a second free parameter to the model, namely a minimum absorption depth, $AD_{\rm min}$, which is expected when an optically thick cloud layer is present at high altitude. For these two additional parameters, we find that $AD_{\rm min} = 1.4452 \pm 0.0016\%$ and $\Delta AD = 0.031\% \pm 0.007\%$. In this model, fit to the data again constrains the pressure at zero altitude to be lower than ~15 mbar. Since the sodium line profile is pressure broadened, a lower pressure at reference altitude requires a far higher sodium abundance to fit the blue tail of the absorption line profile. Using this lower limit for the pressure, we find that the sodium abundance must be $X(\mathrm{NaI}) = 1.5 \times 10^{-5}$ which is 10 times the solar abundance. In addition, the lower pressure at zero altitude also constrains the pressure at which the core of the sodium line is detected to be below $\sim 10^{-6}$ bar; this is a very low pressure at which all atomic sodium should have disappeared through ionization by UV flux, even at lower altitude (Fortney et al. 2003). A fit to the data using a cloud layer and a "Balmer jump" therefore requires a high sodium abundance at significant height in the atmosphere where sodium is believed to be ionized. The "Balmer jump" scenario thus appears to be unlikely.

We conclude that Rayleigh scattering is probably the simplest and most robust interpretation of the data because the absorption-depth curve from 3000 to 6000 Å, including the rise between 4000 and 5000 Å, can be interpreted by means of Rayleigh scattering and a sodium abundance close to solar. In contrast, the "Balmer jump" would require two additional components and a high sodium abundance.

3.2.2. Atomic lines

We considered another alternative to Rayleigh scattering by the addition of plausible atomic lines to interpret the increase

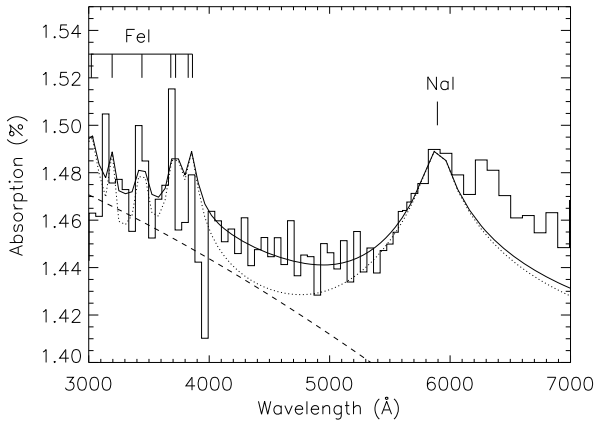

Fig. 4. A similar plot to Fig. 1, with fit including absorption by atomic iron lines. When the atomic iron lines are included, a satisfactory fit to the data can be obtained assuming a lower pressure of ∼15 mbar and larger abundance for sodium and iron of about 10 times solar abundances. The dotted line shows the absorption depth obtained neglecting the Rayleigh scattering. This demonstrates that even with large iron abundance, the Rayleigh scattering has a significant contribution to the absorption depth level between 4000 and 5000 Å, imposing a minimum pressure at the corresponding altitude.

in absorption depth at the shortest wavelengths below 5000 Å (Barman 2007). Taking into account the species abundances, the strongest atomic lines in the 3000−5000 Å wavelength range are those of Ca I, Fe I, Al I, and Cr I. Since the strong calcium line at 4230 Å is not observed, the abundance of atomic calcium must be extremely low. The same conclusion applies to aluminium at 3950 Å and to chromium at 4270 and 3600 Å. These species cannot be responsible for the observed absorption at short wavelengths.

Nonetheless, atomic iron presents a series of strong lines from 2900 to 3860 Å. When the atomic iron lines are included, a satisfactory fit to the data is achieved when we assume (i) a lower pressure of ∼15 mbar; (ii) a higher abundance of both sodium and iron, of about 10 times solar abundance; and (iii) very low calcium, aluminium, and chromium abundances (Fig. 4). The higher sodium abundance is required to fit the blue wing of the line profile, because the line is pressure-broadened, and the pressure is lower.

Calculating the best fit solution with and without iron lines (Figs. 1 and 4), we find similar differences between the data and fit with $\chi^2 = 40$ for 52 degrees of freedom in both cases. This does not favor either one of the two models. However, the model without lines of atomic iron is preferred because it does not require the large ten times solar abundance for sodium and iron. As for calcium, chromium and magnesium, iron is supposed to be trapped in hydrogen compound such as FeH. Because iron has the highest condensation temperature, it is not expected to be present in the gas phase in the absence of other species.

4. Discussion

It is noteworthy that the temperature is found to be relatively high compared to first estimates obtained from secondary transits measurements (Deming et al. 2005). However, a detailed model is needed to interpret the estimated brightness temperature obtained from secondary transits and to determine the pressure and altitude at which this temperature corresponds (Burrows et al. 2005). The temperature obtained here, mainly constrained by the slope of the Rayleigh scattering, is consistent with temperature-pressure profiles obtained by some detailed models of the atmosphere of HD 209458b which provides high temperatures up to 2000 K at 100 mbar, in the night side (Burrows et al. 2006). However, other models to interpret secondary transits measurements provide lower temperatures (Seager et al. 2005) and lower temperature gradients in the millibars pressure domain (Iro et al. 2005; Fortney et al. 2006). Nonetheless, a wide range of models are consistent with the data, and although efforts were made to consider the widest range possible (Seager et al. 2005), measurements remain limited and their interpretation is model-dependent, despite significant recent progress (Knutson et al. 2007; Burrows et al. 2007a).

As shown above, the temperature estimates, in the Rayleigh regime, relies mainly on the slope and, therefore, on the absorption depth measured in the 3000−4000 Å range, where noise is the highest. Nevertheless, a fit to only measurements for absorption depth above 4000 Å provides also a high temperature of $T_0 = 2350 \pm 300$ K (1-σ) at zero altitude. Therefore, although the temperature given in Sect. 3 must be considered in light of its large associated error bars, a high temperature is also required to explain the variation in absorption depth between 4000 and 5000 Å where error bars are the lowest. In addition, this is consistent with the temperature required to explain the high sodium abundance below the sodium condensation level (Sing et al. 2008b).

This fit, which uses only measurements above 4000 Å, strengthens the Rayleigh interpretation. The variation in absorption depth between 4000 and 5000 Å cannot be explained by the absorption in the Balmer series, while the extrapolation of the 4000−5000 Å measurements assuming Rayleigh scattering perfectly matches the absorption depth measured between 3000 and 4000 Å.

Importantly, even if Rayleigh scattering is not detected and the observed increase in absorption depth is due to another phenomenon, such as the Balmer jump (Ballester et al. 2007) or atomic lines (Barman 2007), the present calculations provide a strong upper limit to the pressure at the absorption depth level of 1.453%. The result of Sect. 3 shows that at this level, the pressure must be equal to or smaller than 33 mbar, a pressure at which because of Rayleigh scattering a grazing line of sight becomes optically thick at 4300 Å.

The red wing of the magnesium line at 2850 Å could also explain the increase in absorption depth at the shortest wavelengths, however the abundances of both sodium and magnesium would have to exceed approximately ∼20 times solar. We therefore conclude that the increase in absorption depth at the shortest wavelengths is best explained by Rayleigh scattering. This represents the first direct detection of the main constituent of the planetary atmosphere: molecular hydrogen.

5. Conclusion

Before, the determination of the planetary radius-pressure relationship was missing although this is needed to determine absolute abundances. Until now, many models have relied on the assumption that pressure at the mean planet transit radius is close to 1 bar. Using Rayleigh scattering, we now determine that this pressure should be ∼30 mbar. Even if the Rayleigh scattering does not dominate the absorption, the pressure must be lower than ∼30 mbar. Consequently, the radius of HD 209458b at 1 bar is determined to be about 1.29 Jupiter radius, slightly lower than previously assumed. However, the difference is not sufficient to

explain the puzzling large radius of HD 209458b (Guillot et al. 2006; Burrows et al. 2007b; Chabrier et al. 2007).

In the near future, the new generation of instruments with increased capabilities in the near UV should enable the physical properties of a constantly increasing list of transiting extrasolar planets to be determined. When Rayleigh scattering by H_2 in these planets is detected, it will provide the reference baseline for the determination of the absolute abundances of all the elements to be detected using absorption spectroscopy (Ehrenreich et al. 2006). Measurement of the atmospheric composition will become an increasingly important tool to help understand the origin and nature of extrasolar planets, as increasingly smaller extrasolar planets are detected (Gillon et al. 2007).

Acknowledgements. We warmly thank Drs. G. Ballester, F. Bouchy, D. Ehrenreich, R. Ferlet and G. Hébrard for enlightening discussions. We also thank the referee, Dr. J. Fortney, for his constructive and fruitful remarks.

References

Asplund, M., Grevesse, N., & Sauval, A. J. 2005, ASP Conf. Ser., 336, 25
Ballester, G. E., Sing, D. K., & Herbert, F. 2007, Nature, 445, 511
Barman, T. 2007, ApJ, 661, L191
Brown, T. M. 2001, ApJ, 553, 1006
Burrows, A., Hubeny, I., & Sudarsky, D. 2005, ApJ, 625, L135
Burrows, A., Sudarsky, D., & Hubeny, I. 2006, ApJ, 650, 1140
Burrows, A., Hubeny, I., Budaj, J., Knutson, H. A., & Charbonneau, D. 2007a, ApJ, 668, L171
Burrows, A., Hubeny, I., Budaj, J., & Hubbard, W. B. 2007b, ApJ, 661, 502
Chabrier, G., & Baraffe, I. 2007, ApJ, 661, L81
Charbonneau, D., Brown, T. M., Noyes, R. W., & Gilliland, R. L. 2002, ApJ, 568, 377
Deming, D., Seager, S., Richardson, L. J., & Harrington, J. 2005, Nature, 434, 740
Ehrenreich, D., Tinetti, G., Lecavelier des Etangs, A., Vidal-Madjar, A., & Selsis, F. 2006, A&A, 448, 379
Ehrenreich, D., Lecavelier des Etangs, A., Hebrard, G., et al. 2008, A&A, 483, 933
Fortney, J. J. 2005, MNRAS, 364, 649
Fortney, J. J., Sudarsky, D., Hubeny, I., et al. 2003, ApJ, 589, 615
Fortney, J. J., Cooper, C. S., Showman, A. P., Marley, M. S., & Freedman, R. S. 2006, ApJ, 652, 746
Gillon, M., Pont, F., Demory, B.-O., et al. 2007, A&A, 472, L13
Guillot, T., Santos, N. C., Pont, F., et al. 2006, A&A, 453, L21
Hubbard, W. B., Fortney, J. J., Lunine, J. I., et al. 2001, ApJ, 560, 413
Iro, N., Bézard, B., & Guillot, T. 2005, A&A, 436, 719
Knutson, H. A., Charbonneau, D., Noyes, R. W., Brown, T. M., & Gilliland, R. L. 2007, ApJ, 655, 564
Lecavelier des Etangs, A. 2007, A&A, 461, 1185
Lecavelier des Etangs, A., Pont, F., Vidal-Madjar, A., & Sing, D. 2008, A&A, 481, L83
Seager, S., & Sasselov, D. D. 2000, ApJ, 537, 916
Seager, S., Richardson, L. J., Hansen, B. M. S., et al. 2005, ApJ, 632, 1122
Sing, D. K., et al. 2008a, ApJ, submitted [arXiv:0802.3864]
Sing, D. K., et al. 2008b, ApJ, submitted [arXiv:0803.1054]
Vidal-Madjar, A., Lecavelier des Etangs, A., Désert, J.-M., et al. 2003, Nature, 422, 143
Vidal-Madjar, A., Désert, J.-M., Lecavelier des Etangs, A., et al. 2004, ApJ, 604, L69
Vidal-Madjar, A., Lecavelier des Etangs, A., Désert, J.-M., et al. 2008, ApJ, 676, L57